Biointerface Research in Applied Chemistry
Open-Access Journal (ISSN: 2069-5837)

Article
Volume 13, Issue 3, 2023, 239
https://doi.org/10.33263/BRIAC133.239

Substituted Pyrimidine-Sulfonamide Derivatives: Computational, Synthesis, Characterization, Anti-bacterial, MTT and Molecular Docking Assessment

Mohammad Arshad [1,*], Vasyl Matiychuk [2]

[1] College of Medicine, Shaqra University, Zip Code: 11911, Al-Dawadmi, Saudi Arabia; mohdarshad1985@gmail.com (M.A.);
[2] Ivan Franko National University of Lviv, 6 Kyryla and Mefodia, Zip Code: 79005, Lviv, Ukraine; v_matiychuk@ukr.net (V.M.);
* Correspondence: mohdarshad1985@gmail.com (M.A);

Scopus Author ID 57226619316
Received: 20.12.2022; Accepted: 27.01.2022; Published: 6.06.2022

Abstract: A series of 4-[2-Amino-6-(3, 4, 5-substituted-phenyl) pyrimidin-4-yl]benzenesulfonamide (1-6) was designed and assessed for bioactivity score and physicochemical analysis. All derivatives (1-6), possessed a very good bioactivity score and followed Lipinski's rule of five. Synthesis, structural confirmation, and antibacterial therapeutic assessment were performed, and the findings displayed a very good agreement between the computational and antibacterial findings. Besides, this MTT assay was also carried out against HepG2 cells and represented that more than 95 % of the cells' viability at 3.125 µM was estimated for all members of the series (1-6). The synthesized compounds (1-6) were screened for molecular docking analysis against the receptor L-glutamine: D-fructose-6-phosphate amidotransferase (Glc-N-6P). The findings portrayed that all the compounds possessed minimum binding energy and acted as very good inhibitors of GlcN-6P.

Keywords: pyrimidine derivatives, drug-likeness, antibacterial and physicochemical properties

1. Introduction

Microbial infections and their treatments at the current level are a great obstacle in many countries (developing) [1]. The development of resistance is one of the reasons, and due to that, more than 700,000 deaths/annum have been reported worldwide [2]. The side effects and the resistance by the drug of choice for microbial infections like ciprofloxacin, amoxicillin, and norfloxacin foisted many issues [3]. The continuous escalation in MDR (multi-drug resistance) species makes the investigation of new antimicrobial therapeutic agents compulsory [4]. The compounds with heteroatom have been assessed a lot because of their enormous biological activities [5-7]. The bioactivity of the compounds possessing the pyrimidine moiety has been reported as an antimicrobial (antifungal, antibacterial, antiviral, anti-HIV, anti-tubercular, and antimalarial) analgesic, anti-inflammatory, anti-neoplastic, central nervous system (CNS) depressant, anti-tumor, Bruton's tyrosine kinase (BTK) inhibitors, cardiovascular agents, human A2A adenosine receptor, diuretic, hypnotic drugs for the nervous system, calcium channel blockers [8-15]. Besides this, the derivatives containing SO2N-functional group exhibited enormous biological activities [16]. The recent study is aimed at

design, computational analysis, synthesis, characterization, and antimicrobial and cytotoxicity studies of pyrimidine derivatives with SO2N- functionality.

2. Materials and Methods

Chem Draw Ultra 8.0 and Molinspiration software were used for designing and calculating the drug-likeness and physicochemical properties. The chemicals like guanidine hydrochloride, isopropyl alcohol, sodium hydroxide, ethyl alcohol, 4-acetylbenzenesulfonamide, aldehydes, and other chemicals were purchased from Sigma-Aldrich, Germany. The instruments Melt-Temp and Heraeus Vario EL III analyzer were used for recording the melting points and elemental composition, respectively. The instruments Perkin-Elmer model 1600 FT-IR RX1, Bruker Avance 300 MHz spectrometer, and Micromass Quattro II triple quadrupole mass spectrum was employed to record the FT-IR spectra, NMR (^{1}H or ^{13}C), and mass spectra, respectively. Thin layer chromatographic plates were applied to monitor the reaction status. For assessment of antibacterial potential and percent viability of the cells, the nutrient agar and antibiotic agar, ciprofloxacin, dimethylsulfoxide, MTT, DMEM, FBS were purchased from HIMEDIA, Sigma Aldrich, and HyClone Laboratories, Logan, UT, USA. The antibacterial study was performed using the disc diffusion method and carried out under a laminar flow cabinet, and ELISA recorded the percent viability of the cells following the MTT assay protocol.

2.1. Computational study.

The prediction of bioactivity score and the physicochemical properties was carried out by Molinspiration software (available online at www.molinspiration.com). Structures of the compounds were drawn on ChemDraw Ultra 8.0 and copied as smiles and used for calculating the properties (Bioactivity score and physicochemical) by Molinspiration software [17-28].

2.2. Chemistry.

2.2.1.General procedure for the synthesis of compounds 1-6.

An equimolar ratio of the compounds A1-A6 [17] and guanidine hydrochloride was taken in a round bottom flask and dissolved in isopropyl alcohol. The mixture was set on refluxing for 8 h. On completion of the reaction, the precipitate was observed that was filtered, dried under vacuum, and recrystallized.

2.2.3. Antimicrobial activity assessment.

The strains of the pathogens [*S. aureus* (ATCC-25923), *S. epidermidis* (ATCC-29887), *E. coli* (ATCC-25922), *P. mirabilis* (ATCC-25933)] were sub-cultured in the medium (nutrient agar) and employed for screening the antimicrobial potential by disc diffusion protocol [29-36]. To obtain a suspension of 105 CFU/mL, the bacterial cells were suspended to the McFarland protocol in solution (Saline). The suspension was added equally to the antibiotic agar and transferred to the agar plate under laminar flow. The stock solution was prepared by dissolving 1 mg of each test compound in 100 ml of DMSO, and the paper disc was dipped into this solution and kept on the agar plate to observe the zone of inhibition. Minimum inhibitory concentration, the smallest concentration of the compounds that can arrest the growth of the pathogen, was assessed by the macro dilution method applying the standard

inoculum of CFU/mL, serial dilutions were obtained to the final concentrations 400, 200, 100, 50, 12.5, 6.25 and 3.125µg/ml. Ciprofloxacin was employed as a reference drug in the screening to compare the results of tested components.

2.2.4. Percent viability of the assessment of the cell by the MTT assay.

The HepG2 (Human hepatocellular carcinoma) cells were used to assess the percent viability of cells against the test compounds. The cell lines were cultured in DMEM (Dulbecco's modified Eagle's medium) with 10% FBS (fetal bovine serum) (heat-inactivated), 100 units/mL penicillin,100mg/mL streptomycin, and 2.5mg/mL amphotericin B, at 37 ^{0}C in a saturated humidity atmosphere containing 95% air/5% CO2. Each experiment was recorded in triplicate, and MTT assay was performed by Mossman protocol [37-39].

2.2.5. Molecular docking:

The docking studies were performed using Aautodock-tools 1.5.6, Autodock-vina, and Pymol software utilizing the GlcN-6P-synthase (PDB: 2VF5). According to the protocol mentioned [40-43], the structures of the synthesized compounds were drawn with the help of ChemDraw Ultra 8.0 and optimized for energy to give 3D structures (PDBs).

3. Results and Discussion

The structures of the derivatives 4-[2-amino-6-(4-substituted-phenyl)-pyrimidin-4-yl]benzenesulfonamide (1-6) were designed with the help of ChemDraw Ultra 8.0 software to produce the smiles files. These files were then utilized to calculate the bioactivity score and the physicochemical properties. Bioactivity score or the drug-likeness score (more than zero) corresponded to an active drug molecule, and the results exhibited that all the designed compounds (1-6) were found in the zone for active drug molecule. The Lipinski's rule of five for a standard drug molecule stated that (milogP) (−0.4 to +5.6), (TPSA) (<160 A2), (Natoms) (20 to 70) 4(MW) (180 to 500 D), (nON) (nON ≤ 10), (nOHNH) (≤ 5), (Nviolations) (≤1), (Nrotb) (≤ 10), (Volume) (≤ 500 A3). The physicochemical analysis reported that the designed compounds exhibited agreement with Lipinski's rule of five except for two compounds (5 & 6) that violate the rules Table-1 and Table-2.

Table 1. Representing the physicochemical properties of the derivatives (1-6) and ciprofloxacin.

Physicochemical property score	Compound number						
	1	**2**	**3**	**4**	**5**	**6**	**Ciprofloxacin**
[1](milogP) (−0.4 to +5.6)	2.13	1.72	2.13	1.59	1.10	0.81	-0.701
[2](TPSA) (<160 A^2)	121.21	130.44	121.21	132.20	152.43	172.66	74.569
[3](Natoms) (20 to 70)	25	27	25	24	25	26	24.0
[4](MW) (180 to 500 D)	356.41	386.43	356.41	342.38	358.38	374.38	331.347
[5](nON) (nON ≤ 10)	7	8	7	7	8	9	6
[6](nOHNH) (≤ 5)	4	4	4	5	6	7	2
[7](Nviolations) (≤1)	0	0	0	0	1	1	0
[8](Nrotb) (≤ 10)	4	5	4	3	3	3	3
[9](Volume) (≤ 500 A^3)	298.10	323.65	298.10	280.57	288.59	296.61	285.46

Partition coefficient (1), Total Polar surface area (2), Number of atoms (3), Molecular weight (4), Number of H-bond acceptors (5), Number of H-bond donors (6), Number of violations (7), Number of rotatable bonds (8), Molecular volume (9).

Table 2. Representing the bioactivity score of the designed compounds (1-6) and ciprofloxacin.

S. No.	BIOACTIVITY SCORE					
	GPCR ligand	**Ion channel modulator**	**Kinase inhibitor**	**Nuclear receptor ligand**	**Protease inhibitor**	**Enzyme inhibitor**
1	-0.01	-0.21	0.26	-0.24	-0.03	0.22
2	-0.02	-0.20	0.28	-0.26	-0.07	0.21
3	-0.03	-0.19	0.26	-0.29	-0.08	0.19
4	0.08	-0.10	0.36	-0.10	0.03	0.33
5	0.07	-0.10	0.36	-0.12	0.01	0.33
6	0.05	-0.09	0.37	-0.14	0.02	0.35
Ciprofloxacin	0.12	-0.04	-0.07	-0.19	-0.20	0.20

The bioactive compounds (1-6) were then approached for synthesis by the scheme represented in Figure-1.

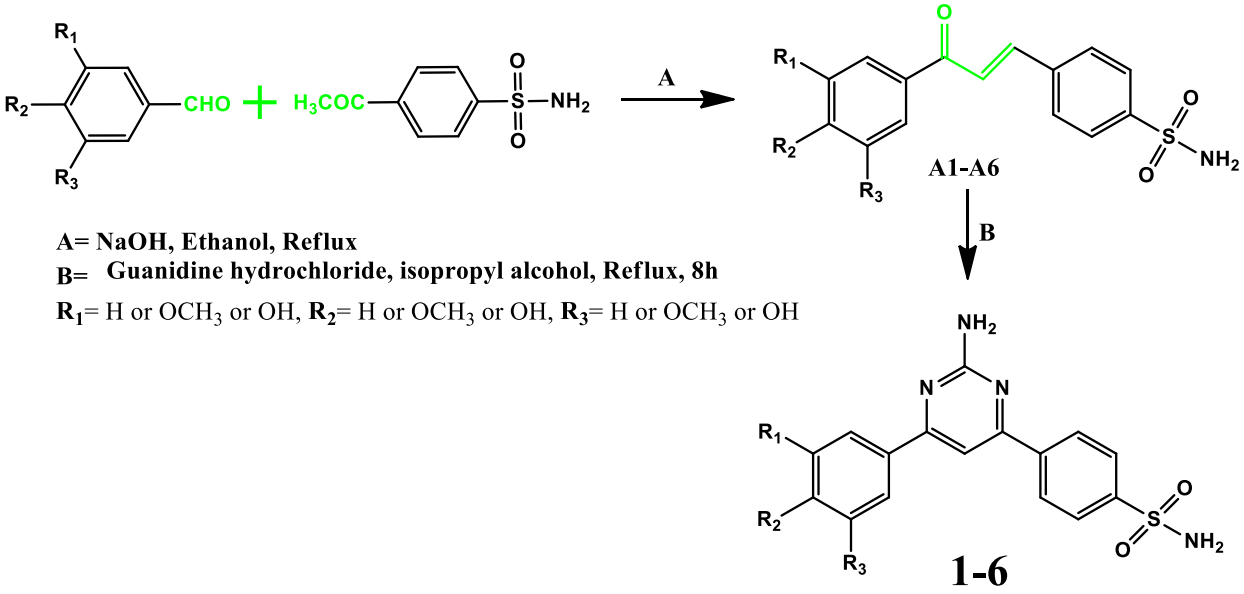

Figure 1. The schematic diagram for the route adopted for the synthesis of compounds (1-6).

Previously synthesized chalcones [17], A1-A6 were reacted with guanidine hydrochloride in isopropyl alcohol to yield compounds 1-6. All the compounds were then undergone structural confirmation by spectroscopic methods such as FTIR, NMR (^{1}H or ^{13}C), and mass spectra, Table-4. The presence of FT-IR bands around 3310-3321 cm^{-1}, 1611-1655 cm^{-1}, 2814-2823 cm^{-1}, and 3330-3381 cm^{-1} due to the NH_2, C=N, OCH_3, and OH functional groups in the structure. Besides these, some other bands were observed around 1045-1071 cm^{-1}, 1027-1034 cm^{-1}, 1578-1589 cm^{-1}, and 3263-3290 cm^{-1} due to functional groups C-N SO_2-Sym, SO_2-Asym, and NH_2 that further confirmed the formation of the compounds (1-6). 1H-NMR spectra for the derivatives (1-6) portrayed the presence of characteristic singlet at 8.165-8.244 ppm due to the NH_2 proton and the disappearance of the singlet due to HC=CH α-β unsaturated protons of the chalcone A1-A6 confirmed the synthesis of compounds (1-6). Besides this, other singlets around 3.721-3.795 ppm, 5.524-5.722 ppm, and 7.542-5.722 ppm were also observed due to OCH3, OH, and SO2-NH2. Further confirmation was performed by ^{13}C-NMR, and the characteristic signal was observed around 57.88-59.25 ppm, 164.92-170.25 ppm due to the presence of OCH3 and C=N in the structures. After structural analysis, the derivatives (1-6) were then screened for antimicrobial potential and percent viability assays using the disc diffusion method and MTT assay. The strains of the pathogens [*S. aureus* (ATCC-25923), *S. epidermidis* (ATCC-29887), *E. coli* (ATCC-25922), *P. mirabilis* (ATCC-25933)] were used in the antimicrobial study. The pathogens were subcultured in nutrient agar

medium and treated with the 5 mm paper discs poured into the solution (one gm of test compounds in DMSO) and calculated the MIC & inhibition zone. The detailed results for the zone of inhibition (mm) and MIC are reported in Table-3 and Figure-2.

Table 3. Representing the zone of inhibition and minimum inhibitory concentration of the synthesized compounds (1-6), ciprofloxacin was used as standard and DMSO as a negative control.

S.No.	Diameter of the halo zone, mm & Minimum Inhibitory Concentration (MIC)							
	Gram-positive				Gram-negative			
	S. aureus		*S. epidermidis*		*E. coli*		*P. mirabilis*	
	Zone of inhibition	*MIC*	*Zone of inhibition*	*MIC*	*Zone of inhibition*	*MIC*	*Zone of inhibition*	*MIC*
1	20.15±0.13	6.25	20.20±0.24	3.12	21.26±0.26	6.25	20.18±0.22	12.5
2	20.37±0.24	6.25	19.30±0.16	3.12	21.30±0.28	6.25	21.10±0.33	12.5
3	20.32±0.18	6.25	20.63±0.20	3.12	21.35±0.30	6.25	22.20±0.26	12.5
4	21.26±0.20	6.25	21.35±0.30	3.12	21.12±0.20	6.25	22.37±0.30	12.5
5	21.43±0.19	6.25	21.37±0.32	3.12	21.33±0.10	6.25	22.55±0.27	12.5
6	21.53±0.33	6.25	22.58±0.27	3.12	23.78±0.28	6.25	22.88±0.25	12.5
Cipro	21.39±0.21	6.25	22.87±0.37	3.12	23.69±0.81	6.25	22.34±0.21	12.5

Table 4. Representing the experimental data and the structures of the compounds.

Compounds	Experimental Data
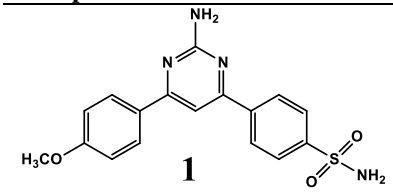 **1**	Yield: 78 %; m. p. 92-94 ^{0}C: Yellow crystals; Anal. calc. for $C_{17}H_{16}N_4O_3S$: C 57.29, H 4.52, N 15.72, found C 57.29, H 4.52, N 15.72; FT-IR (cm^{-1}): 1030 (SO_2-sym), 1051 (C-N), 1060 (C-N), 1578 (SO_2-asym), 1611 (C=N), 1627 (C=N), 2817 (OCH_3), 2992 (CH-Ar), 3263 (NH_2), 3315 (NH_2); ^{1}H NMR (DMSO-d6) (ppm): 3.736 (s, H, OCH_3), 6.960-7-000 (m, 4H, CH-Ar), 7.485 (s, 1H, CH-Ar), 7.580-7.650 (m, 4H, CH-Ar), 7.852 (s, 2H, SO_2NH_2), 8.178 (s, 2H, NH_2); ^{13}C NMR (DMSO-d6) (ppm): 58.18 (OCH_3), 124.11, 124.56, 128.37, 128.93, 129.66, 130.53, 131.77, 132.90, 132.59, 133.35, 136.19, 136.56, 138.88, 138.43, 165.48 (C=N), 169.34(C=N); ESI-MS (m/z): [M^+ + 1]: 357.10 (357.25).
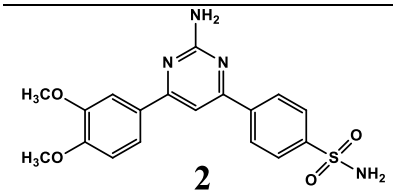 **2**	Yield: 80 %; m. p. 95-97 ^{0}C: Yellow crystals; Anal. calc. for $C_{18}H_{18}N_4O_4S$: C 55.95, H 4.70, N 14.50, found 55.95, H 4.70, N 14.50; FT-IR (cm^{-1}): 1027 (SO_2-sym), 1047 (C-N), 1059 (C-N), 1580 (SO_2-asym), 1619 (C=N), 1625 (C=N), 2821 (OCH_3), 2814(OCH_3), 2989 (CH-Ar), 3261 (NH_2), 3310 (NH_2); ^{1}H NMR (DMSO-d6) (ppm): 3.721 (s, H, OCH_3), 3.795 (s, H, OCH_3), 6.782-7.091 (m, 3H, CH-Ar), 7.438-7.490 (m, 4H, CH-Ar), 7.532 (s, 2H, SO_2NH_2), 7.608 (s, 1H, CH-Ar), 8.244 (s, 2H, NH_2); ^{13}C NMR (DMSO-d6) (ppm): 57.88 (OCH_3), 59.02 (OCH_3), 123.22, 124.08, 124.89, 125.39, 125.78, 126.77, 129.20, 129.93, 132.10, 132.56, 132.92, 134.45, 134.80, 135.67, 135.99, 164.92 (C=N), 169.90 (C=N); ESI-MS (m/z): [M^+ + 1]: 387.11 (387.27).
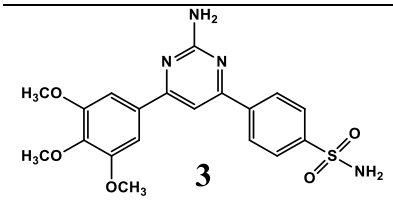 **3**	Yield: 82 %; m. p. 91-93 ^{0}C: Yellow crystals; Anal. calc. for $C_{19}H_{20}N_4O_5S$: C 54.80, H 4.84, N 13.45, found C 54.80, H 4.84, N 13.45; FT-IR (cm^{-1}): 1032 (SO_2-sym), 1045 (C-N), 1063 (C-N), 1585 (SO_2-asym), 1627 (C=N), 1620 (C=N), 2815 (OCH_3), 2820 (OCH_3), 2823 (OCH_3), 2999 (CH-Ar), 3272 (NH_2), 3312 (NH_2); ^{1}H NMR (DMSO-d6) (ppm): 3.757 (s, H, OCH_3), 3.774 (s, H, OCH_3), 3.788 (s, H, OCH_3), 6.851-6.968 (m, 2H, CH-Ar), 7.618 (s, 1H, CH-Ar), 7.760-7.815 (m, 4H, CH-Ar), 7.859 (s, 2H, SO_2NH_2), 8.188 (s, 2H, NH_2); ^{13}C NMR (DMSO-d6) (ppm): 57.90 (OCH_3), 59.23 (OCH_3), 59.25 (OCH_3), 124.66, 125.70, 127.17, 127.84, 129.30, 135.27, 135.39, 136.49, 136.83, 137.08, 137.67, 139.70, 139.95, 140.19, 140.66, 165.22 (C=N), 170.25 (C=N); ESI-MS (m/z): [M^+ + 1]: 417.12 (417.18).
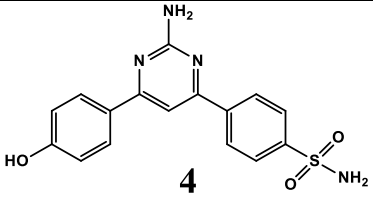 **4**	Yield: 85 %; m. p. 90-92 ^{0}C: Yellow crystals; Anal. calc. for $C_{16}H_{14}N_4O_3S$: C 56.13, H 4.12, N 16.36, found 56.13, H 4.12, N 16.36; FT-IR (cm^{-1}): 1028 (SO_2-sym), 1050 (C-N), 1068 (C-N), 1581 (SO_2-asym), 1633 (C=N), 1640 (C=N), 2993 (CH-Ar), 3267 (NH_2), 3321 (NH_2), 3381 (OH); ^{1}H NMR (DMSO-d6) (ppm): 5.613 (s, H, OH), 7.012-7.188 (m, 4H, CH-Ar), 7.315-7.410 (m, 4H, CH-Ar), 7.508 (s, 1H, CH-Ar), 7.547 (s, 2H, SO_2NH_2), 8.199 (s, 2H, NH_2); ^{13}C NMR (DMSO-d6) (ppm): 125.87, 126.51, 127.44, 127.93, 128.10, 130.22, 131.91, 132.13, 132.79, 133.09, 136.25, 136.87, 138.09, 138.55, 166.19 (C=N), 169.67 (C=N); ESI-MS (m/z): [M^+ + 1]: 343.08 (343.15).
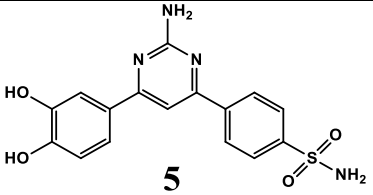 **5**	Yield: 81 %; m. p. 94-96 ^{0}C: Yellow crystals; Anal. calc. for $C_{16}H_{14}N_4O_4S$: C 53.62, H 3.94, N 15.63, found C 53.62, H 3.94, N 15.63; FT-IR (cm^{-1}): 1034 (SO_2-sym), 1049 (C-N), 1071 (C-N), 1589 (SO_2-asym), 1630 (C=N), 1635 (C=N), 2995 (CH-Ar), 3290 (NH_2), 3319 (NH_2), 3345 (OH), 3372 (OH); ^{1}H NMR (DMSO-d6) (ppm): 5.524 (s, H, OH), 5.621 (s, H, OH), 7.140-7.219 (m, 3H, CH-Ar), 7.421-7.514 (m, 4H, CH-Ar), 7.594 (s, 1H, CH-Ar), 7.780 (s, 2H, SO_2NH_2), 8.165 (s, 2H, NH_2); ^{13}C NMR (DMSO-d6) (ppm): 123.14, 123.88, 124.11, 125.27, 125.17, 126.44, 129.31, 129.79, 132.21, 132.83, 132.98, 134.10, 134.69, 135.55; 135.88, 165.70 (C=N), 169.89 (C=N); ESI-MS (m/z): [M^+ + 1]: 359.08 (359.15).
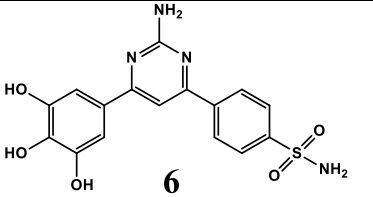 **6**	Yield: 86 %; m. p. 97-99 ^{0}C: Yellow crystals; Anal. calc. for $C_{16}H_{14}N_4O_5S$: C 51.33, H 3.77, N 14.97, found C 51.33, H 3.77, N 14.97; FT-IR (cm^{-1}): 1035 (SO_2-sym), 1047 (C-N), 1070 (C-N), 1587 (SO_2-asym), 1635 (C=N), 1629 (C=N), 3012 (CH-Ar), 3285 (NH_2), 3320 (NH_2), 3330 (OH), 3342 (OH), 3355 (OH); ^{1}H NMR (DMSO-d6) (ppm): 5.608 (s, H, OH), 5.632 (s, H, OH), 5.722 (s, H, OH), 6.912-6.988 (m, 2H, CH-Ar), 7.142-7.253 (m, 4H, CH-Ar), 7.482 (s, 1H, CH-Ar), 7.567 (s, 2H, SO_2NH_2), 8.180 (s, 2H, NH_2); ^{13}C NMR (DMSO-d6) (ppm): 125.19, 125.90, 127.00, 127.61, 129.55, 135.11, 135.79, 136.18, 136.60, 137.00, 137.43, 139.17, 139.77, 140.10, 140.80,165.59 (C=N), 169.02 (C=N); ESI-MS (m/z): [M^+ + 1]: 375.07 (375.14).

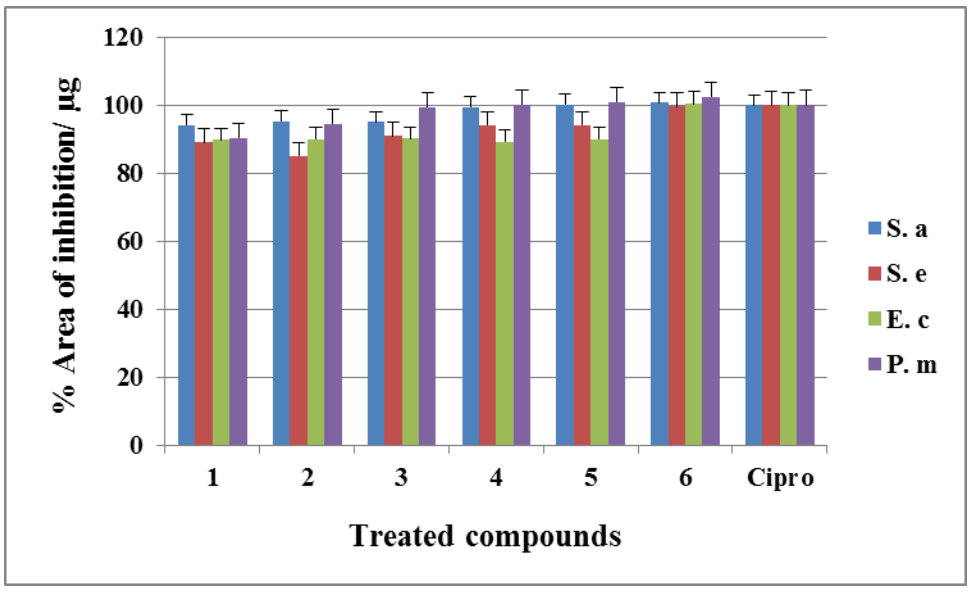

Figure 2. Representing the percent area of inhibition per microgram of the test compounds (1-6) and ciprofloxacin.

The antimicrobial screening results portrayed that all the compounds (1-6) possessed significant antimicrobial potential and were found in strong agreement with the computational findings. The percent viability assay of all the synthesized derivatives was screened against the HepG2 cells, the HepG2 cells were treated with the increasing concentration of the compounds (1-6), and estimated the % viability of the cells at 48 h incubation, Figure-3. The MTT assay findings revealed that more than 90 percent of the viability of the cells was observed at 3.125 µM.

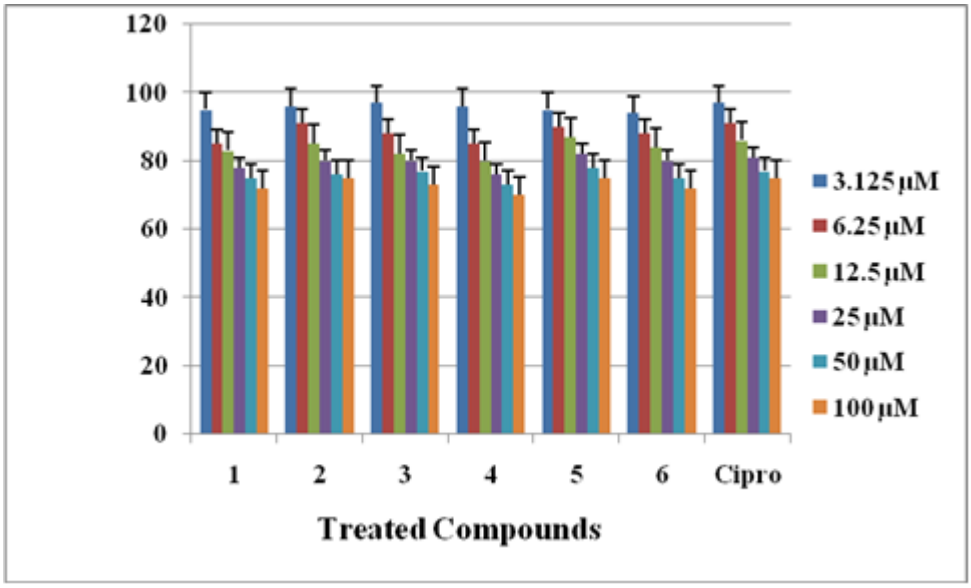

Figure 3. Representing the percent viability of cells at a different concentration range of the test compounds (1-6) against HepG2 cells.

3.1. Molecular docking study.

The results of in vitro antibacterial screening prompted us to perform molecular docking analysis to compare the in vitro and in silico findings. The molecular docking for the synthesized derivatives (1-6) and the ciprofloxacin was carried out on the receptor protein GlcN-6P synthase (PDB: 2VF5), and the findings are represented in Figure-5.

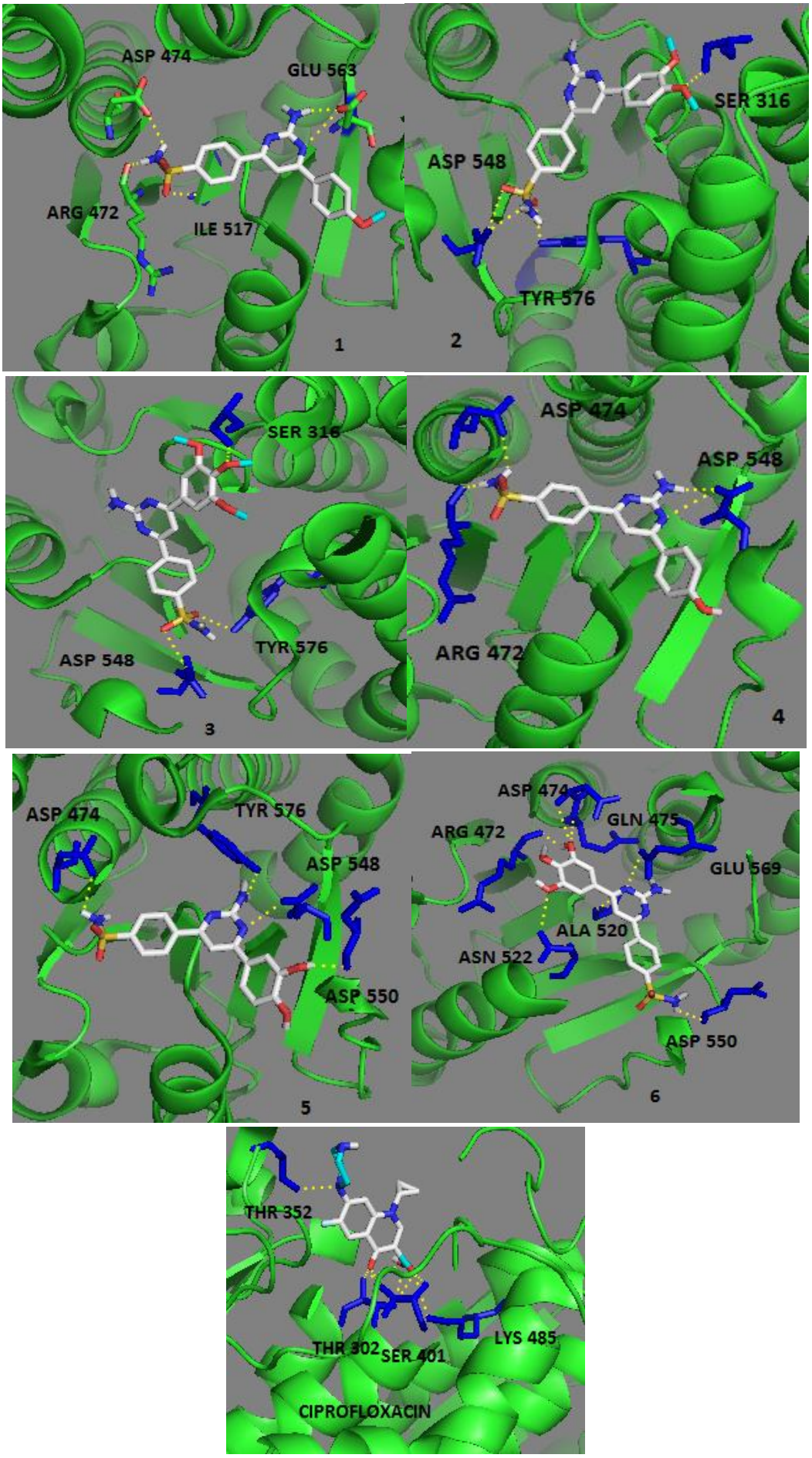

Figure 4. Representing the docking images of the synthesized compounds (1-6) and ciprofloxacin with the receptor GlcN-6P-synthase.

The compounds were observed to have the H-bonding with various amino acids like ASP 474, ARG 472, ILE 517, GLU 567, ASP 548, SER 316, ASP 550, TYR 576, GLN 475, ALA 520, GLU 569, ASN 522. The most bioactive compound (6) of the series was observed to possess the H-bonding ASP 474, ARG 472, ASP 550, GLN 475, ALA 520, GLU 569, ASN 522. Some compounds of the series represented the common H-bonding with (1, 4, 5 & 6), TYR 576 (2, 5 & 3), ASP 548 (2, 4 & 5), ASP 550 (5 & 6), ARG 472 (1 & 4), SER (2 & 3). On the other hand, ciprofloxacin was observed to have H-bonding with VAL 567 and TYR 576. On comparing the results, it was also observed that three compounds of the series (2, 5 & 3) had the H-bonding with TYR 576. The findings were observed in the strong recommendation of the experimental results and other computational findings (Figure-4).

4. Conclusions

The computational analysis for drug-likeness exhibited that the derivative with OCH_3 substitution was found to have the bioactivity score in the zone for the active drug molecule as an enzyme inhibitor and kinase inhibitor, while on the other hand, the derivative with OH substitution exhibited the zone for the active drug in terms of enzymes inhibitor, a kinase inhibitor, protease inhibitor, and GPCR ligand. The structures of the synthesized compounds were confirmed using spectroscopic methods. The significant antibacterial potential was exhibited by all the synthesized compounds and strongly recommended the computational results. It was observed that compound number six was the most active member of the series. As per the MTT assay observations, all synthesized compounds observed more than 95 % viability of the cells at 3.125 µM by all the synthesized compounds. Additionally, the molecular docking analysis represented that all the compounds possessed minimum binding energy and acted as a good inhibitor of GlcN-6P.

Funding

This research received no external funding

Acknowledgments

Dr. Mohammad Arshad is highly thankful to Dr. Feras Almarshad, the Dean and the research ethics committee, College of Medicine Al-Dawadmi, Shaqra University, Kingdom of Saudi Arabia, for their cooperation in accomplishing this work (Grant No. CMD/DWD/SU/2020/10/032)

Conflicts of Interest

The authors declare no conflict of interest.

References

1. Lopez, H.; Li, J.Z.; Balan, D.A.; Willke, R.J.; Rittenhouse, B.E.; Mozaffari, E.; Vidal, G.; Zitto, T.; Tang, T. Hospital resource use and cost of treatment with linezolid versus teicoplanin for treatment of serious gram-positive bacterial infections among hospitalized patients from South America and Mexico: Results from a multicenter trial. *Clinical Therapeutics* **2011,** *25*, 1846-1871, https://doi.org/10.1016/S0149-2918(03)80173-X.
2. Babu, K.R.; Eeshwaraiah, B.; Aravind, D.; Harshadas, M. M.; Rallabaldi, M. R.; Apurba, B.; Rakeshwar, B. Synthesis of Quinoline Analogs: Search for Antimalarial Agents. *Monatsh. Chem*. **2008,** *139*, 179-181, https://doi.org/10.1007/s00706-007-0772-5.

3. Khan, S.A.; Asiri, A.M.; Alamry, K.A.; El-Daly, S.A.; Zayed, M.A.M. Eco-friendly synthesis and in vitro antibacterial activities of some novel chalcones. *Russ. J. Bioorg. Chem.* **2013,** *39,* 353-357, https://doi.org/10.1134/s1068162013030072.
4. York, A. Historical influences on antibiotic resistance. *Nat. Rev. Microbiol.* **2017,** *15,* 576-577, https://doi.org/10.1038/nrmicro.2017.111.
5. Kalaria, P N.; Karad. S. C.; Raval, D. K. A review on diverse heterocyclic compounds as the privileged scaffolds in antimalarial drug discovery. *Eur. J. Med. Chem.* **2018,** *158,* 917-936, https://doi.org/10.1016/j.ejmech.2018.08.040.
6. Bhat, A. R.; Arshad, M.; Lee, E. J.; Pokharel, S.; Choi, I.; Athar, F. Synthesis, Characterization, and Anti-Amoebic Activity of N-(Pyrimidin-2-yl)benzenesulfonamide Derivatives. *Chem. Biodivers.* **2013,** *10,* 2267-2277, https://doi.org/10.1002/cbdv.201300009.
7. Arshad, M.; Bhat, A. R.; Hoi, K. K.; Choi, I.; Athar, F. Synthesis, characterization and antibacterial screening of some novel 1,2,4-triazine derivatives. *Chin. Chem. Lett.* **2017,** *28,* 1559-1565, https://doi.org/10.1016/j.cclet.2016.12.037.
8. Kamal, A.; Dastagiri, D.; Janaki, M.; Ramaiah, Reddy, J. S.; Bharathi, E. V.; Reddy, M. K.; Sagar M.V. P.; Reddy, T. L.; Pushpavalli, S.N.C.V.L., Pal-Bhadra M. Synthesis and apoptosis inducing ability of new anilino substituted pyrimidine sulfonamides as potential anticancer agents. *Eur. J. Med. Chem.* **2011,** *46,* 5817-5824, https://doi.org/10.1016/j.ejmech.2011.09.039.
9. Arshad, M.; Bhat, A. R.; Pokharel, S.; Lee, E. J.; Athar, F.; Choi, I. Synthesis, characterization and anticancer screening of some novel piperonyl–tetrazole derivatives. *Eur. J. Med. Chem.* **2014,** *71,* 229-236, https://doi.org/10.1016/j.ejmech.2013.11.008.
10. Liu, H.; Qu, M.; Xu, L., Han, X.; Wang, C.; Shu, X.; Yao, J.; Liu,K.; Peng, J.; Li, Y.; Ma, X. Design and synthesis of sulfonamide-substituted diphenylpyrimidines (SFA-DPPYs) as potent Bruton's tyrosine kinase (BTK) inhibitors with improved activity toward B-cell lymphoblastic leukemia. *Eur. J. Med. Chem.* **2017,** *135,* 60-69, https://doi.org/10.1016/j.ejmech.2017.04.037.
11. Sayed, M. T.El.; Hussein, H.A.R.; Elebiary, M.; Ghada, N.; Hassan, S.; Elmessery, S.M.; Elsheakh, A. R.; Nayel M.; Abdel-Aziz, H.A. Design and synthesis of sulfonamide-substituted diphenylpyrimidines (SFA-DPPYs) as potent Bruton's tyrosine kinase (BTK) inhibitors with improved activity toward B-cell lymphoblastic leukemia. *Biorg. Chem.* **2018,** *78,* 312-323, https://doi.org/10.1016/j.bioorg.2018.03.009.
12. Fang, Z.; Zheng, S.; Chan, KF.; Yuan, W.; Guo, Q.; Wu, W.; Lui, HK.; Lu, Y.; Leung, YC.; Chan,TH.; Wong, KY.; Sun, N. Design, synthesis and antibacterial evaluation of 2,4-disubstituted-6-thiophenyl-pyrimidines. *Eur. J. Med. Chem.* **2018,** *161,* 141-153, https://doi.org/10.1016/j.ejmech.2018.10.039.
13. Kumar, S.; Singh, J.; Narasimhan, B.; Shah, SAA.; Lim, SM.; Ramasamy, K.; Mani, V. Reverse pharmacophore mapping and molecular docking studies for discovery of GTPase HRas as promising drug target for bis-pyrimidine derivatives. *Chem. Cent. J.* **2018,** *12,* 1-11, https://doi.org/10.1186/s13065-018-0475-5.
14. Ghith, A.; Youssef, KM.; Ismail, NSM.; Abouzid, KAM. Design, synthesis and molecular modeling study of certain VEGFR-2 inhibitors based on thienopyrimidne scaffold as cancer targeting agents. *Bioorg Chem.* **2018,** *83,* 111-128, https://doi.org/10.1016/j.bioorg.2018.10.008.
15. Hassaneen H.M.; Saleh F.M.; Abdallah T.A.; Mohamed M.F.; Mohamed Y.S.; Awad E.M.; Abdelhamid I.A. Synthesis, Cytotoxicity, Antimicrobial and Docking Simulation of Novel Pyrazolo[3,4-d]pyrimidine and pyrazolo[4,3-e][1,2,4]triazolo[3,4-c] pyrimidine Derivatives. *Mini Rev Med Chem.* **2018,** *19,* 657-670, https://doi.org/10.2174/1389557518666181017162459.
16. Wani, M. Y.; Bhat, A.R.; Azam, A.; Choi, I.; Athar, F. Probing the antiamoebic and cytotoxicity potency of novel tetrazole and triazine derivatives. *Eur. J. Med. Chem.* **2012,** *48,* 313-320, https://doi.org/10.1016/j.ejmech.2011.12.033.
17. Arshad. M. Synthesis, characterization, and antimicrobial assessment of some computationally bioactive 1,2-oxazole derivatives. Synthesis, Characterization, and Antimicrobial Assessment of Some Computationally Bioactive 1,2-Oxazole Derivatives. *Russ. J. Gen. Chem.* **2018,** *88,* 1886-1891, https://doi.org/10.1134/S1070363218090207.
18. Horishny, V. Ya.; Arshad, M.; Matiychuk. V. S. Synthesis and Anticancer Activity of 2-Cyano-*N*-(furan- 2-ylmethyl)-2-(4-oxo-3-arylthiazolidin-2-ylidene)acetamide Derivatives. *Russ. J. Org. Chem.* **2021,** *57,* 212-218, https://doi.org/10.1134/S1070428021020111.
19. Lipinski, CA.; Lombardo, F.; Dominy, BW.; Feeney, PJ. Experimental and computational approaches to estimate solubility and permeability in drug discovery and development settings. *Adv Drug Deliv Rev.* **1997,** *23,* 3-26, https://doi.org/10.1016/S0169-409X(00)00129-0.
20. Chaban, T.; Arshad, M.; Kostyshyn, L.; Drapak I.; Matiychuk, V. Synthesis, molecular docking and antimicrobial activities 2-(1-allyl-1*h*-tetrazol-5-ylsulfanyl)-n-(aryl)acetamides. *Eur. Chem. Bull.* **2021,** *10,* 230-236, https://doi.org/10.17628/ECB.2021.10.230-236.
21. Myrko, I.; Chaban, T.; Matiichuk, Y.; Arshad M.; Matiychuk, V. Approaches for the synthesis, chemical modification and biological properties of N-acylphenothiazines. *Current Chemistry Letters* **2021,** *10,* 377-392, https://doi.org/10.5267/j.ccl.2021.5.005.

22. Alodeani, E. A.; Arshad, M.; Izhari, M.A. Anti-uropathogenic activity, drug likeness, physicochemical and molecular docking assessment of (E-)-N'-(substitutedbenzylidene)-2-(quinolin-8-yloxy) acetohydrazide. *Asian Pac J Trop Biomed.* **2015,** *5,* 676-683, https://doi.org/10.1016/j.apjtb.2015.04.010.
23. Arshad, M.; Khan, M.S.; Nami, S.A.A. Synthesis, characterization, biological and molecular docking assessment of computationally bioactive 1, 3-thiazolidin-4-one derivatives bearing indole and bi-pyrimidine moieties. *Journal of the Iranian Chemical Society* **2021,** *18,* 2397-2406, https://doi.org/10.1007/s13738-021-02200-4.
24. Arshad, M.; Khan, M.S.; Nami, S.A.A.; Ahmad, S. I.; Kashif, M.; Anjum, A. Synthesis, characterization, biological, and molecular docking assessment of bioactive 1,3-thiazolidin-4-ones fused with 1-(pyrimidin-2-yl)-1H-imidazol-4-yl) moieties. *Journal of the Iranian Chemical Society* **2021,** *18,* 1713-1727, https://doi.org/10.1007/s13738-020-02144-1.
25. Arshad, M.; Khan, M.S.; Nami, S.A.A. Norfloxacin analogues: Drug likeness, synthesis, biological, and molecular docking assessment. *Russ. J. Bioorg.c Chem.* **2021,** *47,* 483-495; https://doi.org/10.1134/S1068162021020047.
26. Arshad, M.; Shoeb Khan, M.; Asghar Nami, S.A.; Ahmad D. Synthesis, Characterization, Computational, Antimicrobial Screening, and MTT Assay of Thiazolidinone Derivatives Containing the Indole and Pyridine Moieties. *Russ J Gen Chem*. **2018,** *88*, 2154-2162, https://doi.org/10.1134/S1070363218100213.
27. Arshad, M.; Khan, M.S.; Nami, S.A.A. Synthesis, Biological Activity, and Molecular Docking Assessment of Some New Sulfonylated Tetrazole Derivatives. *Russ J Gen Chem*. **2019,** *89,* 1851-1858, https://doi.org/10.1134/S1070363219090202.
28. Arshad, M.; Ahmad D.; Akhter, R. 1, 3-thiazolidin-4-one derivatives bearing pyrimidine moieties: Design, computational studies, synthesis, characterization, antimicrobial, MTT assessment and molecular docking assessment. *Chemical Data Collections* **2020,** *28,*100405, https://doi.org/10.1016/j.cdc.2020.100405.
29. Arshad, M. Design, computational, synthesis, characterization, antimicrobial, MTT and molecular docking assessment of bipyrimidine derivatives possessing indole moiety. *Journal of the Iranian Chemical Society* **2020,** *17,* 1305-1315, https://doi.org/10.1007/s13738-020-01855-9.
30. Arshad, M.; Khan, M.S.; Nami, S.A.A.; Ahmad D. (E)-Substituted-N-((1,3-diphenyl-1H-pyrazol-4-yl)methylene)benzeneamine: synthesis, characterization, antibacterial, and MTT assessment. *SN Appl. Sci.* **2019,** *1,* 548-559, https://doi.org/10.1007/s42452-019-0571-8.
31. Iram, N.E.; Khan, M. S.; Jolly, R.; Arshad, M.; Alam, Alam, P.; Khan, R. H.; Firdaus, F. Interaction mode of polycarbazole–titanium dioxide nanocomposite with DNA: Molecular docking simulation and in-vitro antimicrobial study. *Journal of Photochemistry and Photobiology B: Biology* **2015,** *153,* 20-32; https://doi.org/10.1016/j.jphotobiol.2015.09.001.
32. Nami, S. A. A.; Arshad, M.; Shakir, M.; Khan, M. S.; Alam, M.; Lee, D-U.; Park, S.; Sarikavakli, N.; Morphological, structural, molecular docking and biocidal studies of newly synthesized Ppy-MA/TiO2 nanocomposites. *Polymers for advanced technology* **2015,** *26,* 1627-1638, https://doi.org/10.1002/pat.3591.
33. Nami, S. A. A.; Khan, M. S.; Arshad, M.; Raza M. A.; Khan, I.; Spectral, morphological, and antibacterial studies of conducting copolymers, Ppy-MA, and their nanocomposites, Ag@Ppy-MA. *Polymers for advanced technology* **2017,** *28,* 10-19, https://doi.org/10.1002/pat.3846.
34. Kareem, A.; Laxmi; Arshad M.; Nishat, N. Herbo-Mineral based Schiff base ligand and its metal complexes: synthesis, characterization, catalytic potential and its biological applications. *Journal of Photochemistry and Photobiology B: Biology* **2016,** *160,* 163-171, https://doi.org/10.1016/j.jphotobiol.2016.03.030.
35. Alaqeel, S. I.; Almansour, A. I.; Arumugam, N.; Kumar, R. S.; Ponmurugan, K.; Al-Dhabi, N. A. Antimicrobial activities of novel class of dispirooxindolopyrrolidine grafted indanedione hybrid heterocycles against carbapenemase producing Klebsiella pneumoniae (CKP). *Journal of Infection and Public Health* **2021,** *14*, 1870-1874, https://doi.org/10.1016/j.jiph.2021.10.023.
36. Sánchez-López, A. L.; Perfecto-Avalos, Y.; Sanchez-Martinez, A.; Ceballos-Sanchez, O.; Sepulveda-Villegas, M.; Rincón-Enríquez, G.; Rodríguez-González, V.; Garcia-Varela, R.; Lozano, L. M.; Navarro-López, D.E.; Sanchez-Ante, G.; Corona-Romero, K.; López-Mena, E.R. Influence of erbium doping on zinc oxide nanoparticles: Structural, optical and antimicrobial activity. *Applied Surface Science* **2022,** *575,* 151764, https://doi.org/10.1016/j.apsusc.2021.151764.
37. Mosmann, T. Rapid colorimetric assay for cellular growth and survival: Application to proliferation and cytotoxicity assays. *J. Immunol. Methods* **1983,** *65,* 55-63, https://doi.org/10.1016/0022-1759(83)90303-4.
38. Michael, D.S.; Priya, M.K.; Sidharthan, J.; Kumar, M.; Solomon, R.V.; Jonathan, D.R. Synthesis, crystallography, DFT, MTT assay, and molecular docking studies of an exocyclic double-bonded crystalline chalcone. *Chemical Data Collections* **2021,** *36,* 100773, https://doi.org/10.1016/j.cdc.2021.100773.
39. Soltan-Dallal, M.M.; Validi, M.; Douraghi, M.; Fallah-Mehrabadi, J.; Lormohammadi, L. Evaluation the cytotoxic effect of cytotoxin-producing Klebsiella oxytoca isolates on the HEp-2 cell line by MTT assay. *Microbial Pathogenesis* **2017,** *113,* 416-420, https://doi.org/10.1016/j.micpath.2017.11.003.
40. Morris, GM.; Goodsell, DS.; Halliday, RS.; Huey, R.; Hart, W.E.; Belew, R.K.; Olson, A.J. Automated docking using a Lamarckian genetic algorithm and an empirical binding free energy function. *J Comput Chem.* **1998,** *19,* 1639-1662, https://doi.org/10.1002/(SICI)1096-987X(19981115)19:14%3C1639::AID-JCC10%3E3.0.CO;2-B.

41. Mouilleron, S.; Badet-Denisot, MA.; Golinelli-Pimpaneau B. Ordering of C-terminal loop and glutaminase domains of glucosamine-6-phosphate synthase promotes sugar ring opening and formation of the ammonia channel. *J Mol Biol.* **2008,** *377*, 1174-1185, https://doi.org/10.1016/j.jmb.2008.01.077.
42. Trott, O.; Olson, A. J. AutoDock Vina: improving the speed and accuracy of docking with a new scoring function, efficient optimization and multithreading, *J Comput Chem.* **2010,** *31*, 455-461, https://doi.org/10.1002/jcc.21334.
43. Arshad, M. Heterocyclic compounds bearing pyrimidine, oxazole and pyrazole moieties: design, computational, synthesis, characterization, antibacterial and molecular docking screening. *SN Appl. Sci.* **2020,** *2*, 467-475, https://doi.org/10.1007/s42452-020-2243-0.